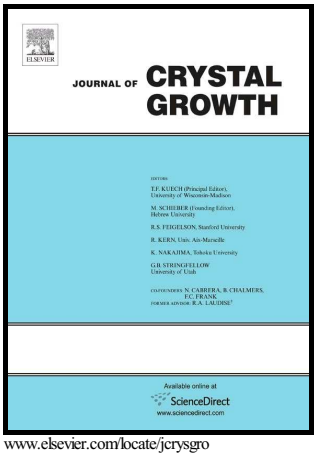

www.elsevier.com/locate/jcrysgro

Study on Nucleation Kinetics of Lysozyme Crystallization

Chen Lin, Yang Zhang, Jing J Liu, Xue Z Wang

PII: S0022-0248(16)30621-2
DOI: http://dx.doi.org/10.1016/j.jcrysgro.2016.10.028
Reference: CRYS23667

To appear in: *Journal of Crystal Growth*

Cite this article as: Chen Lin, Yang Zhang, Jing J Liu and Xue Z Wang, Study or Nucleation Kinetics of Lysozyme Crystallization, *Journal of Crystal Growth* http://dx.doi.org/10.1016/j.jcrysgro.2016.10.028

Study on Nucleation Kinetics of Lysozyme Crystallization

Chen Lin[1], Yang Zhang[1], Jing J Liu[1] and Xue Z Wang[1,2,*]

[1] School of Chemistry and Chemical Engineering, South China University of Technology, Guangzhou 510640, China

[2] School of Chemical and Process Engineering, University of Leeds, Leeds LS2 9JT, U.K.

*** Correspondence author:**
Professor Xue Z. Wang

School of Chemistry and Chemical Engineering
South China University of Technology
381 Wushan Rd, Tianhe District
Guangzhou, PR China 510640
Tel: +86 20 8711 4000, Fax: +86 20 8711 4000
Email; xuezhongwang@scut.edu.cn

&

Personal Chair in Intelligent Measurement and Control
Institute of Particle Science and Engineering
School of Chemical and Process Engineering
University of Leeds
Leeds LS2 9JT, UK
Tel +44 113 343 2427, Fax +44 113 343 2384, Email x.z.wang@leeds.ac.uk

Abstract

The nucleation kinetics of hen egg-white lysozyme crystallization was investigated using a hot stage cooling crystallizer and a microscope to monitor the solution crystallization process in real time. Images of crystals were continuously recorded under varied precipitant and protein concentrations. The nucleation rate was found to be higher at higher precipitant concentration, and increase monotonically with protein concentration if the precipitant concentration was held

constant. Attempt was made to interpret the experimental data using classical nucleation theory. It was found that the model predictions are lower than the experimental values at low supersaturations but agree well with experimental data at high supersaturations. The trends in the experimental data suggest that two nucleation mechanisms might co-exist: heterogeneous nucleation seeming to be the dominant at low supersaturation while at higher supersaturation homogeneous nucleation seeming to play the major role.

Keywords: A1. video microscopy; B3. hot stage; B1. lysozyme; A1. crystallization; A1. nucleation kinetics; A1. classical nucleation theory

1. Introduction

Nucleation as the first step of crystallization often dictates the physicochemical properties of the final crystals [1, 2]. It is understood that if the nucleation rate is fast, many nuclei may form in a short time, and growth of the crystals consume solution concentration and may lead to termination of further nucleation. It is likely that at the end, crystals will form with a narrow particle size distribution. On the other hand if the nucleation rate is slow and fewer nuclei would form at the beginning, the supersaturation of solution will drop slowly, which could continue to produce new nuclei and grow to many different sizes with a wide size distribution[3]. However, it is accepted that there is still incomplete knowledge about nucleation.

The classical nucleation theory remains the main framework describing a nucleation phenomenon [2]. According to the theory, the main factors that affect the nucleation rate are the concentration, temperature and surface energy [4]. However there is only limited nucleation kinetic data available in the literature to validate the theory. Some experimental studies were reported to determine nucleation kinetics parameters. Burke and Judge[4, 5] studied nucleation by measuring the number of crystals formed in a batch crystallizer after a while of nucleation but the number of crystals formed was counted at the end, not continuously counted. Galkin and Velilov [6, 7] used a temperature jump method for the determination of nucleation rates. It was also based on counting the number of crystals appearing, but the number was again not continuously measured. Bhamidi [8, 9] studied Hen egg-white lysozyme (HEWL) nucleation and did use a particle counter (PC2000, from Spectrex Corporation), but the technique was not intuitive and could have errors. Bhamidi modeled the data using an empirical kinetic expression

based on the classical nucleation theory. Dixit et al.[10] also compared the nucleation rates to the predictions of classical nucleation theory. They seemed to conclude that the model to predict the number of protein crystals may have uncertainties and may have underestimated the nucleation rates.

In this study, a hot stage – microscope integrated system was applied to study the nucleation rate of hen egg-white lysozyme (HEWL). The system allows the number of crystals formed to be counted in high accuracy and continuously over time. Like in some previous literature, the results are also compared to the prediction of classical nucleation models and the findings are reported. In addition, the crystallization experiments were conducted in much wider initial HEWL supersaturation values and precipitant concentrations than the above reviewed previous studies on HEWL nucleation. In terms of the method of the current study, it is also based on counting the number of crystals, but the difference is that the method is not only accurate (based on counting the number of crystals in an image) but also can continuously monitor the growth. Since both nucleation and growth occur in a crystallizing solution simultaneously, a major problem faced in nucleation kinetics experiments is the separation of nucleation from growth[11, 12]. But it was agreed that detecting crystals during the early stages of growth allows one to obtain nucleation rates [9]. So assuming that every critical nucleus can grow into a crystal, one can obtain the nucleation rate by counting crystals as they are formed[8].

2. Experiment

2.1. Solution preparation

Hen egg-white lysozyme (HEWL) purchased from Sigma-Aldrich was used without additional purification. Sodium chloride (NaCl) was used as the precipitant. The protein and precipitant were dissolved in 0.1 mol/L sodium acetate buffer at pH 4.5. The solution was then filtered through a 0.22 μm filter (Nylon 66). Before each experiment, both the protein solution in sodium acetate buffer (0.1 mol/L) at pH 4.5 and NaCl solution were stored at 20℃ for at least 1h before they were mixed. The final crystallizing batch solution was prepared by mixing protein and precipitant solutions with equal volume. The concentration of lysozyme protein in solution was determined by measuring the UV (UVmini-1240) absorbance at 280 nm using extinction coefficient α^{280nm}=2.64 ml $mg^{-1}cm^{-1}$, as previous researchers did [15].

2.2. Protein solubility and induction time

The solubility of HEWL was measured at 20^0C in solutions of different sodium chloride concentrations (2%, 3%, 4%, 5%, 6%, 7% and 8%, g/ml) in 0.1 mol/L sodium acetate buffer at pH 4.5. Corresponding to each sodium chloride concentration, e.g. 2%, different amounts of HEWL were dissolved in the solution, and at each HEWL concentration three UV spectra were taken and averaged. The absorbance at 280 nm, the characteristic absorbance for HEWL was taken. A model was then developed for prediction of HEWL concentration using UV spectra in a solution corresponding to that sodium chloride concentration. Then at 20^0C, for a solution corresponding to a specific sodium chloride concentration, e.g. 2%, a saturated HEWL solution was made (adding HEWL into the solution until it became opaque), and three UV spectra of the supernatant were taken, and the averaged spectrum was used as the model to prediction a concentration – the solubility. It was observed that the solubility of lysozyme decreases with the increase of NaCl concentration, as depicted in Figure 2. Under the condition of 20℃, the solubility of lysozyme protein was found to be 13.18, 8.58 and 5.76 mg/ml for NaCl concentration of 3%, 4% and 5% respectively. These values were slightly greater than those reported by Cacioppo and Pusey[13]，but similar with the values that reported by Adachi[14]. Because of the different experimental device and measurement method, the error range is understandable and acceptable.

The induction time of HEWL was obtained by measuring the turbidity of the mixed solution using the turbidity probe of Pharmavision Ltd (www.pharmavision-ltd.com). Firstly, the supersaturated solution 20℃ was heated to 30^0C and stirred to make lysozyme completely dissolved and cultivate for 1 hour. Adopting the method of instantaneous cooling, the temperature of the solution was reduced to 20℃. An induction time (t_{ind}) was determined by turbidity which underwent a sudden change at the onset of nucleation. Then the relationship between $\log(t_{ind})$ and $\log(\sigma)$ ($\sigma = c/c^*$), c is the concentration of the protein solution and c^* is the equilibrium concentration), and the nucleation free energy diagram of lysozyme can be obtained.

2.3. Determination of nucleation rates

The experimental setup for the determination of nucleation rates is shown in Figure 1. The supersaturated solution of 30 μl was introduced into a circular quartz crystallizer of radius 0.3 cm. The

circular quartz crystallizer was placed on a hot stage. The temperature of the hot stage was controlled at 20℃ (±0.1℃) by liquid nitrogen. The solution were covered by inert oil to suppress heterogeneous nucleation on the air-solution interface and avoid solvent evaporation, as described in literature [15]. The number density of particles with time can be observed immediately via the microscope (OLYMOUS BX53, magnification 20×) after mixing the protein and NaCl solution. Images of crystals were continuously recorded at a rate of one photo every 30 seconds. Assuming that every nucleus of critical size can grow up as a crystal, one can obtain the nucleation rate by counting crystals manually as they are formed. The nucleation rate can be determined as J=N/(Vt) as reported in literature [7], where J is the nucleation rate , crystal number /(μl.s), V is the volume of the solution (μl), t is the time (s). Nucleation rate is then determined from the slope of a linear plot of number density versus time over an initial period of nucleation. Every experiment under a given condition was replicated five times to verify reproducibility.

3. Results and discussion

3.1. Induction time and nucleation free energy

Figure 3 shows the induction time estimated by measuring the sudden change in turbidity. Different initial HEWL supersaturations will have different induction time. The relationship between $\log t_{ind}$ and $1/(\log\sigma)^2$, where σ is supersaturation and t_{ind} is induction time, is drawn in Figure 4. According to the classical nucleation theory model, the interfacial tension can be estimated through the slope of a straight line between $1/(\log\sigma)^2$ and $\log t_{ind}$ [2]. Figure 4 shows two straight lines, their slopes are 0.3231 over the range of high supersaturation and 0.1694 over the range of low supersaturation. Based on these two slopes, the corresponding surface energies are derived as 0.1131 mJ/m^2 and 0.0912 mJ/m^2 respectively, showing that surface energy decreases with the decrease in protein concentration.

Figure 5 is the nucleation free energy diagram of lysozyme. It illustrates the thermodynamic effects of nucleation and the variation of activation barrier with supersaturation at temperature of 20℃ and NaCl of 5%. The surface contribution ΔGs increases with the crystal nucleus radius r, while the volume contribution ΔGv decreases with r, and Gc increases with r until reaching a critical value which is the critical crystal nucleus free energy ΔGc* and then decreases. It is clear that there is an energetic barrier ΔGc (the nucleation barrier) that must be crossed to induce the formation of stable nuclei. The value of the free energy of the forming cluster also depends on its size, the critical size r_c, any cluster

with a size below r_c will tend to dissolve, while clusters with a size larger than r_c will grow to crystals. This is the reason that if the crystals are formed, the solution must be supersaturated beyond a threshold value. From Figure 5 it is also noticed that the values of r_c and ΔGc^* vary inversely with supersaturation. The energy barrier explains why a solution should experience precipitation under thermodynamic conditions only if a certain value of supersaturation is exceeded. Now it should be clear that nucleation is a probabilistic phenomenon. So we assume that nucleus of the size equal or larger than the critical size can grow into a crystal, one can obtain the nucleation rate by counting crystals as they are forming.

3.2. Nucleation rate

In primary nucleation, nuclei form directly from a supersaturated solution and can grow into crystals. Primary nucleation can occur homogenously or heterogeneously[16]. Supersaturation controls the dominant mechanisms[17]. In this study, the nucleation rate under varied precipitant concentrations and protein supersaturation was measured. Figure 6 shows images of crystals formed in the crystallizer the change with time in number of crystals and crystal morphology can be continuously monitored.

The initial period of time between the creation of supersaturation and the formation of nuclei of critical size is the induction time, a horizontal straight line as shown in Figure 7. Since crystals must first grow to a detectable size after nucleation has occurred, particles may not be detected at very early times. So we assumed that stable nuclei can grow up to crystals that can be counted. With the number of crystals N that appeared in the droplet counted, nucleation rate can be determined.

Figure 7 plots the number of crystals observed vs time. The nucleation rate can be determined as $J=N/(Vt)$ [7], where J is the nucleation rate, i.e. number of nuclei per volume (ml) per second, N the number of crystal observed, V the volume, ml, t time, s. A. At the start of mixing two solutions: lysozyme solution in sodium acetate buffer (0.1 mol/L) at pH 4.5, and the NaCl solution, the supersaturation is high and primary nucleation occurs. As a result of primary nucleation, supersaturation decreases. Reduction in supersaturation reduces the chances of secondary nucleation, and the main process can be considered as growth of the nuclei generated in primary nucleation. On the basis of this, the rate of particle formation, or nucleation rate can be determined by the initial solution conditions.

A series of nucleation rates at different protein concentrations and NaCl concentrations were thus estimated. Figure 8 summarizes the nucleation rate data at 3%, 4% and 5% NaCl respectively as a

function of protein concentration. The experiment results are in agreement with expectations: the nucleation rate increases monotonically with protein concentration at a constant precipitant concentration; and overall, is higher at a higher precipitant concentration. At a high salt concentration, i.e. above 5%, the relationship between nucleation rates and protein concentration was absent in the data because crystals with needle shape were formed along with the expected tetragonal crystals reported by Bhamidi et al[8]. Galkin and Vekilov[6, 7] reported similar deviations in nucleation rates at high salt concentration. So low precipitant concentration was chosen to measure the nucleation rate of lysozyme protein.

3.3. Comparison with predictions using classical nucleation theory

The classical nucleation theory is chosen here to interpret the data. The two-step nucleation theory is not chosen since it relies on the availability of disordered liquid or amorphous metastable clusters in the homogeneous solutions prior to nucleation, but there was no evidence that the system of study here supports the existence of such clusters with properties allowing the nucleation of crystals in them[18]. In fact, it was accepted that the classical nucleation theory still represents the main framework for understanding of nucleation phenomena.

On the basis of the classical nucleation theory, the dependence of the nucleation rate on supersaturation σ and protein molecular concentration C is [19, 20]

$$J = A C \exp\left(-\frac{B}{\ln^2 \sigma}\right) \quad (1)$$

The pre-exponential factor A is a complicated function of the molecular-level kinetics parameters. There have been attempts to analytically derive an expression for this coefficient for nucleation from solution. In all cases, the final formulae for A contains variables that are often impossible to determine independently[21, 22].

The parameter B is related to the thermodynamic barrier for the creation of the critical cluster ΔG_c^* and for a spherical cluster can be written as

$$B = \frac{16\pi}{3} \frac{\nu^2 \gamma^3}{(k_B T)^3} \quad (2)$$

where v is the protein molecular volume in the crystal and γ is the surface free energy of the critical cluster. The values of A and B are shown in Table 1. From the values of B, the surface free energy γ

shown in Table 1 can be estimated.

Figure 9 shows the classical nucleation theory model fit to the data. The fitting result for the parameters A and B were shown in Table 1. It can be seen from Figure 9 that the model agrees reasonably well with experiment data at high supersaturation but deviates from the experimental values at lower supersaturation in all cases. The trend of the fitting results in Figure 9 suggests that the nucleation kinetic data may be divided into two areas depending on supersaturation .

Revised models and the data are shown in Figure 10. Improved agreement between data and model predictions can be seen. The revised models fit to data which split into two regions for different protein supersaturations. The fitting results of parameters A and B were shown in Table 2. Due to parameter B being directly related to the surface energy, the results suggest a lower surface energy at low protein supersaturation. The value of parameter B in the low protein supersaturation region is about half of that in the high protein supersaturation region. Hence, the fitting results indicate that the data can be divided into two regions: a heterogeneous region at lower protein supersaturation and a homogeneous nucleation region at higher protein supersaturation.

On the basis of the classical nucleation theory model, the surface energy of the crystal nuclei can be calculated from the value of the estimated parameter B at temperature of 20℃, using a molecular volume of lysozyme of 2.97×10^{-26} m^3[23]. The calculated surface energy values are shown in Tables 1 and 2. The calculated values of surface energy of nucleation in our experiment are somewhat different from those found by Galkin and Vekilov [7], but nevertheless both are of the same order of magnitude [24, 25]. From Table 2 we can see that a lower surface energy corresponds to low protein supersaturation. When the nucleation rate data is divided into two regions, the surface energy values obtained in the low protein supersaturation range were consistently smaller than those at the high protein supersaturation range. In heterogeneous nucleation, nucleation is induced by solid particles or gas-liquid interface by reducing the surface energy of the formation of crystal nucleui. In homogeneous nucleation, the surface energy between solute clusters and bulk phase is not affected by the solvent in the clusters and gas-liquid interface [24]. The result supports the hypothesis that heterogeneous nucleation seems to be the dominant mechanism at low supersaturation while at higher supersaturation homogeneous nucleation seems to play the major role.

4. Conclusion

The nucleation kinetics of hen egg-white lysozyme (HEWL) crystallization was studied using a hot stage crystallizer and a microscope that can take images in real time. Images of crystals were continuously recorded under varied precipitant and protein supersaturations. It was demonstrated that the number of crystals is strongly correlated to the concentration of lysozyme protein, so controlling the protein concentration in some ways can be used to decouple nucleation from growth. The experimental data and the nucleation kinetics for the model protein system seem following the classical nucleation theory, the nucleation rate depends exponentially on protein supersaturation. It was found that the model predictions agree well with experiment data at high supersaturations but are lower than the experimental values at low supersaturations, the former was not reported before and the later is consistent with what was reported in literature. In addition, with the model fitted by classical nucleation theory, heterogeneous nucleation may be the dominant nucleation mechanism at low protein supersaturation and homogeneous nucleation may be the dominant mechanism at higher protein supersaturation . The technique allows distinction between homogeneous and heterogeneous nucleation and allows determinations the rates of homogeneous nucleation.

Acknowledgements

Financial support from the China One Thousand Talent Scheme, the National Natural Science Foundation of China (NNSFC) under its Major Research Scheme of Mesoscale Mechanism and Control in Multiphase Reaction Processes (project reference: 91434126), the Natural Science Foundation of Guangdong Province (project title: Scale-up study of protein crystallization based on modelling and experiments, project reference: 2014A030313228), as well as the Guangdong Provincial Science and Technology Projects under the Scheme of Applied Science and Technology Research Special Funds (Project Reference: 2015B020232007) is acknowledged.

Reference

[1] M. Ildefonso, N. Candoni, S. Veesler, Using microfluidics for fast, accurate measurement of lysozyme nucleation kinetics, Cryst. Growth Des., 11 (2011) 1527-1530.

[2] J.M. GarcíA-Ruiz, Nucleation of protein crystals, J. Struct. Biol., 142 (2003) 22-31.

[3] P.G. Vekilov, Nucleation, Cryst. Growth Des., 10 (2010).

[4] R.A. Judge, R.S. Jacobs, T. Frazier, The effect of temperature and solution pH on the nucleation of tetragonal lysozyme crystals, Biophys. J . 77 (1999) 1585–1593.

[5] M.W. Burke, R. Leardi, R.A. Judge, M.L. Pusey, Quantifying main trends in lysozyme nucleation: The effect of precipitant concentration, supersaturation, and impurities, Cryst. Growth Des., 1 (2001) 333-337.

[6] O. Galkin, P.G. Vekilov, Are nucleation kinetics of protein crystals similar to those of liquid droplets?, J. Am. Chem. Soc. , 122 (1999) 156-163.

[7] O. Galkin, P.G. Vekilov, Direct determination of the nucleation rates of protein crystals, J. Phys. Chem. B, 103 (1999).

[8] V. Bhamidi, E. Skrzypczak-Jankun, C.A. Schall, Dependence of nucleation kinetics and crystal morphology of a model protein system on ionic strength, J. Cryst. Growth, 232 (2001) 77-85.

[9] V. Bhamidi, A. Sasidhar Varanasi, C.A. Schall, Measurement and modeling of protein crystal nucleation kinetics, Cryst. Growth Des., 2 (2002) 395-400.

[10] N.M. Dixit, A.M. Kulkarni, C.F. Zukoski, Comparison of experimental estimates and model predictions of protein crystal nucleation rates, Colloid Surface A, 190 (2001) 47-60.

[11] G. Tammann, Aggregatzustaende, die zustandsaenderungen der materie in abhaengigkeit von druck und temperature, Second Edition, Von Leopold Voss, Leipzig, (1922) 222-223.

[12] A.A. Chernov, Modern crystallography III crystal growth, in: Springer Series in Solid-State Sciences, Berlin, Heidelberg, Springer Berlin Heidelberg, 1984.

[13] E. Cacioppo, M.L. Pusey, The solubility of the tetragonal form of hen egg white lysozyme from pH 4.0 to 5.4, J. Cryst. Growth, 114 (1991) 286–292.

[14] H. Adachi, A. Niino, K. Takano, H. Matsumura, S. Murakami, T. Inoue, Y. Mori, T. Sasaki, Temperature-screening system for determining protein crystallization conditions, Jpn. J Appl. Phys., 44 (2005) 4080-4083.

[15] O. Galkin, P.G. Vekilov, Nucleation of protein crystals: critical nuclei, phase behavior, and control pathways, J. Cryst. Growth, 232 (2001) 63-76.

[16] R. Lacmann, A. Herden, M. Ch., Kinetics of Nucleation and Crystal Growth, Chem. Eng. Technol., 22 (1999) 279-289.

[17] A. Mersmann, B. Braun, M. Löffelmann, Prediction of crystallization coefficients of the population balance, Chem. Eng. Sci., 57 (2002) 4267-4275.

[18] P.G. Vekilov, The two-step mechanism of nucleation of crystals in solution, Nanoscale, 2 (2010) 2346-2357.

[19] D.T.J. Hurle, Handbook of crystal growth, North-Holland, 1993.

[20] P.G. Vekilov, L.A. Monaco, B.R. Thomas, V. Stojanoff, F. Rosenberger, Repartitioning of NaCl and protein impurities in lysozyme crystallization, Ber. Dtsch. Chem. Ges., 2005 (1996) 670-675.

[21] D. Turnbull, Kinetics of heterogeneous nucleation, J. Chem. Phys., 18 (1950) 198-203.

[22] J.C. Fisher, Rate of nucleation in condensed systems, J. Chem. Phys., 17 (1949) 71-73.

[23] A. Nadarajah, M.L. Pusey, Growth mechanism and morphology of tetragonal lysozyme crystals, Acta Crystallogr., Sect D: Biol. Crystallogr., 52 (1996) 13.

[24] S. Jung-Uk, C. Galder, D.R. Link, T. Todd, J. Yanwei, P. Katie, F. Seth, Control and measurement of the phase behavior of aqueous solutions using microfluidics, J. Am. Chem. Soc., 129 (2007) 8825-8835.

[25] J.U. Shim, G. Cristobal, D.R. Link, T. Thorsen, S. Fraden, Using microfluidics to decouple nucleation and growth of protein crystals, Cryst. Growth Des., 7 (2007) 2192-2194.

Table 1. The fitting result of classical nucleation theory

C_{NaCl}(m/v)	A	B	γ （mJ/m^2）
3%	0.8377	0.5317	0.1335
4%	2.605	1.725	0.1976
5%	7.353	2.576	0.3214

Table 2. The results of model fit to data split into two regions for different NaCl concentration

C_{NaCl}(m/v)	A	B	γ （mJ/m^2）
3%(L)	0.4858	0.3365	0.1146
3%(H)	0.9669	0.6214	0.1406
4%(L)	0.8667	1.040	0.1669
4%(H)	3.205	1.924	0.2049
5%(L)	0.8980	1.402	0.1844
5%(G)	9.698	3.390	0.2475

L—low protein supersaturation H—high protein supersaturation

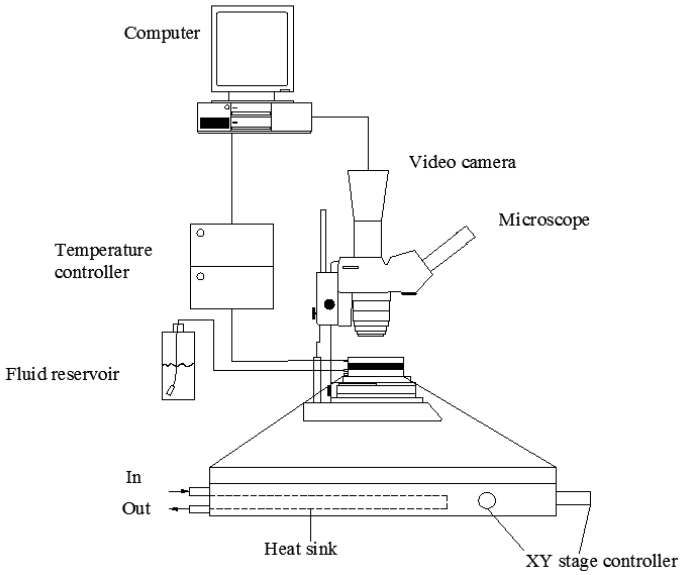

Figure 1. Schematic of the experiment setup

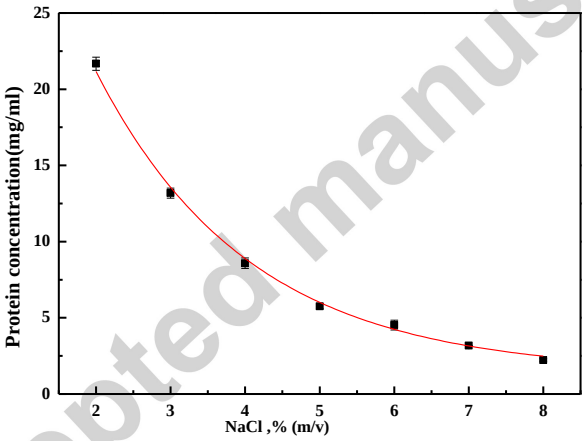

Figure 2. Effect of salt concentration on the solubility of lysozyme at a constant temperature of 20℃.

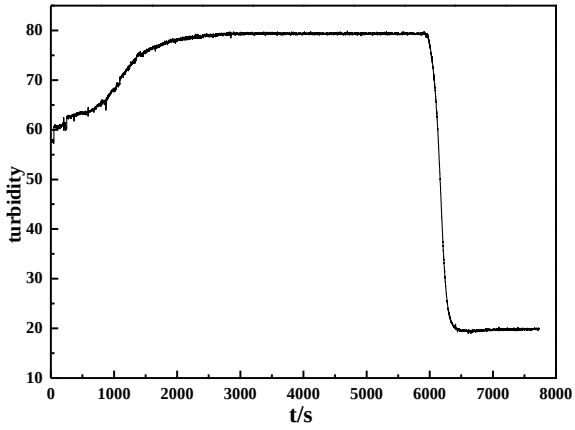

Figure 3. The induction time of HEWL was obtained by measuring the turbidity of the mixed solution using the turbidity probe of Pharmavision Ltd (www.pharmavision-ltd.com).

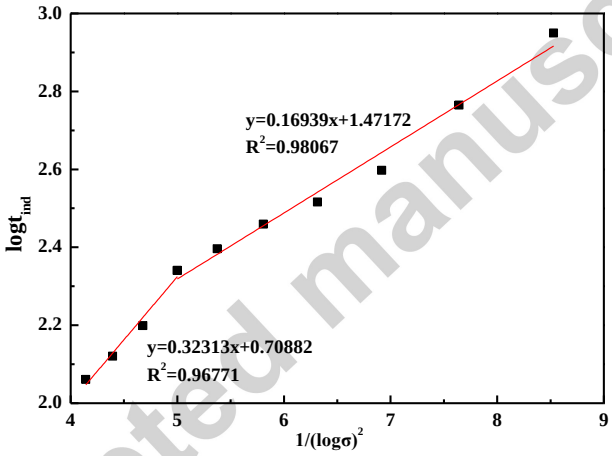

Figure 4. The relationship between $1/(\log\sigma)^2$ and $\log t_{ind}$ with supersaturation at temperature of 20℃ and NaCl of 5%

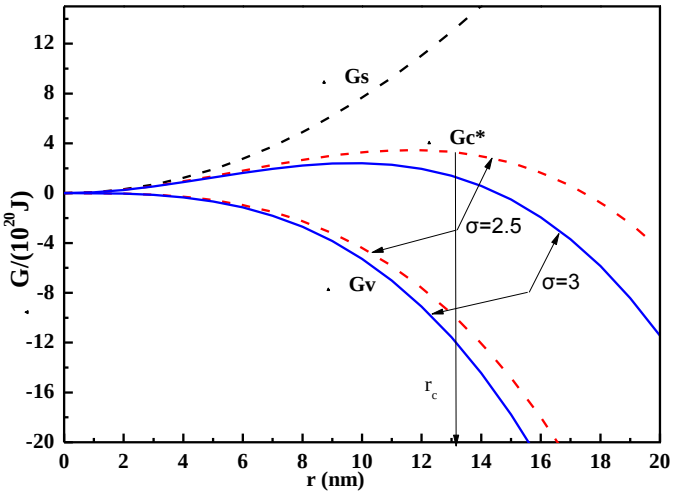

Figure 5. Nucleation free energy diagram of lysozyme. Illustration of the thermodynamic effects of nucleation and the variation of activation barrier with supersaturation at temperature of 20℃ and NaCl of 5%, ΔGs is the surface contribution, ΔGv is the volume contribution, ΔGc* is critical nucleation barrier, r_c is the critical size.

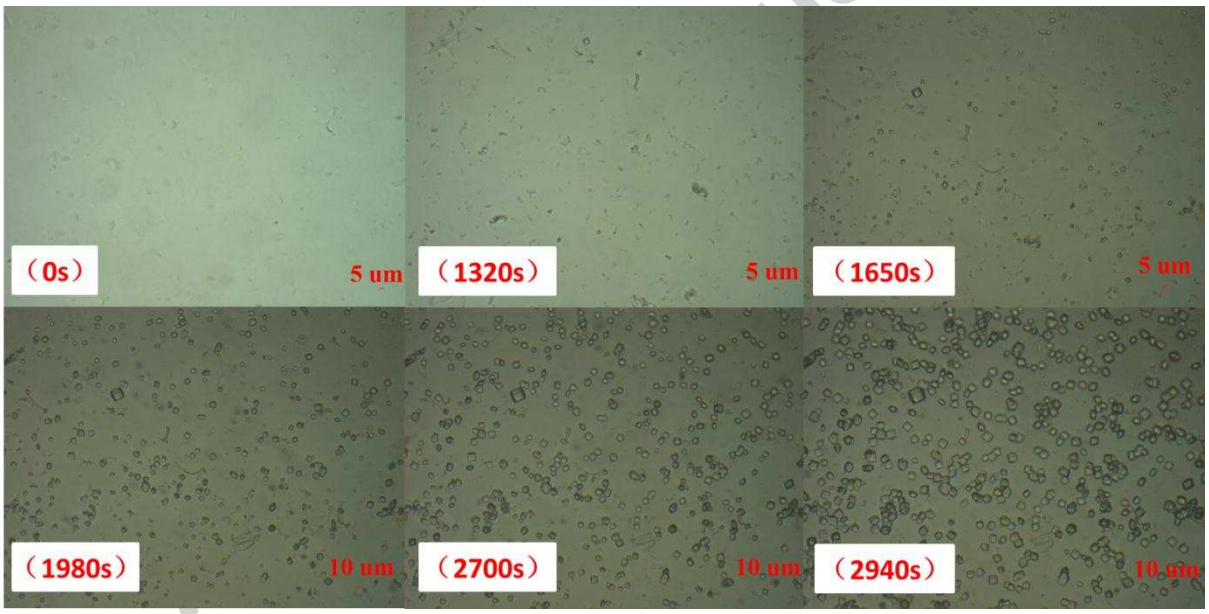

Figure 6. The number of crystals that changed with time in the droplet were monitored by a microscope video in real time. The concentration of lysozyme is 21.09 mg/ml and the precipitant of NaCl is 4%, the temperature is 20℃.

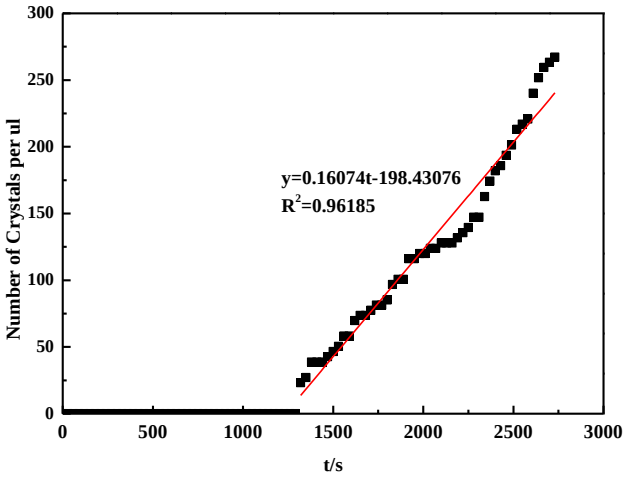

Figure 7. The nucleation rate data at the concentration of lysozyme is 21.09 mg/ml and the precipitant of NaCl is 4%, at 20℃. Number density of particles is plotted against time. The slope during the initial time period gives the nucleation rate.

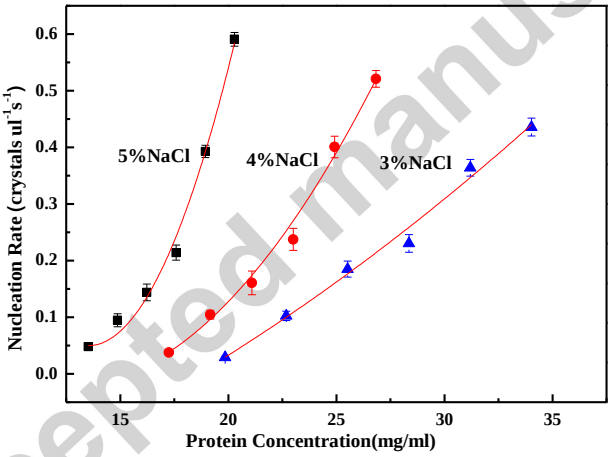

Figure 8. Nucleation rates at various NaCl concentrations of 3%(▲),4%(●) and 5%(■)(w/v) in 0.1M acetate buffer pH=4.5 plotted against protein concentration.

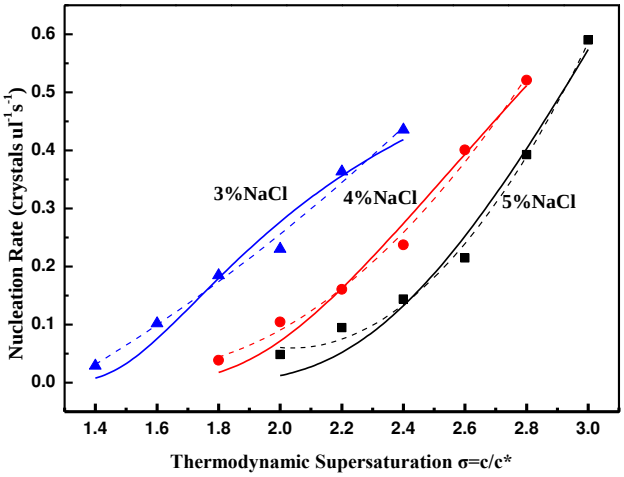

Figure 9. Nucleation rate data versus protein supersaturation plotted at varied NaCl concentrations of 3%(▲),4%(●) and 5%(■)(w/v) in 0.1 M acetate buffer pH=4.5. Solid lines are fit with classical nucleation theory, dashed line are fits with an exponential function.

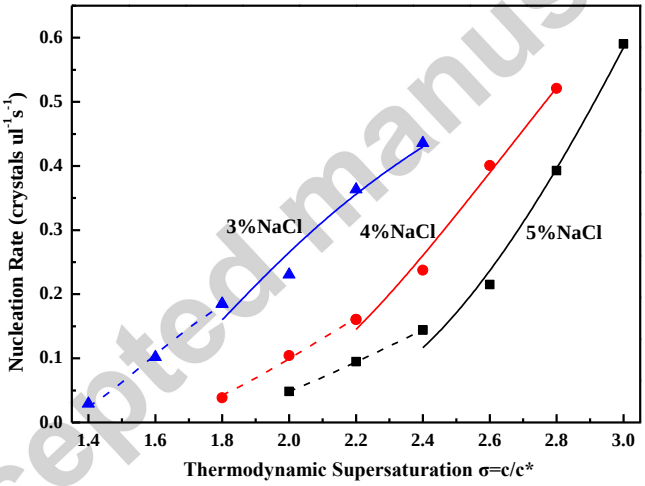

Figure 10. Model fit to data split into two regions for different NaCl concentrations of 3%(▲),4%(●) and 5%(■)(w/v) in 0.1 M acetate buffer pH=4.5. Solid lines belong to homogeneous (high supersaturation) and dashed lines belong to heterogeneous (low supersaturation).

Highlights

1. The nucleation rate of hen egg-white lysozyme crystallization is investigated.

2. The system allows crystal numbers accurately and continuously recorded.

3. At low supersaturation classical nucleation theory gives lower predictions.

4. At high supersaturations classical nucleation gives more accurate predictions.